JOURNAL OF VIROLOGY, Apr. 2000, p. 3709–3714 Vol. 74, No. 8
0022-538X/00/$04.00+0

A Novel Subgenomic Murine Leukemia Virus RNA Transcript Results from Alternative Splicing

JÉRÔME DÉJARDIN,[1] GUILLAUME BOMPARD-MARÉCHAL,[1] MURIEL AUDIT,[1] THOMAS J. HOPE,[2] MARC SITBON,[1] AND MARYLÈNE MOUGEL[1]*

Institut de Génétique Moléculaire de Montpellier, IFR 24, CNRS-UMR5535, and Université Montpellier II, F-34293 Montpellier Cedex 5, France,[1] and Salk Institute for Biological Studies, La Jolla, California 92037[2]

Received 4 October 1999/Accepted 26 January 2000

Here we show the existence of a novel subgenomic 4.4-kb RNA in cells infected with the prototypic replication-competent Friend or Moloney murine leukemia viruses (MuLV). This RNA derives by splicing from an alternative donor site (SD′) within the capsid-coding region to the canonical envelope splice acceptor site. The position and the sequence of SD′ was highly conserved among mammalian type C and D oncoviruses. Point mutations used to inactivate SD′ without changing the capsid-coding ability affected viral RNA splicing and reduced viral replication in infected cells.

The retroviral life cycle requires that significant amounts of RNA remain unspliced and perform several functions in the cytoplasm. Thus, the full-length RNA serves as the viral genetic material that will be encapsidated in viral particles and as the mRNA encoding structural and enzymatic proteins required for viral replication. Simple retroviruses are defined as those viruses which produce one single-spliced *env* RNA from this full-length precursor RNA, whereas complex retroviruses are characterized by the production of multiple spliced RNA species (18). Because *cis*-acting and coding functions in the viral genome frequently overlap, most of the studies on RNA splicing and transport regulation in murine leukemia viruses (MuLV) have been conducted with extensively reshaped retroviral vectors that are replication defective (9, 14, 17). Besides these models with vectors, usage of MuLV canonical or cryptic splice sites has been reported in the context of insertional mutagenesis occurring in animals inoculated with the replication-competent wild-type Moloney MuLV (2, 15, 19, 22, 26). Since such events are accompanied by the rearrangement of both the target cellular proto-oncogene and the inserted proviral DNA (20, 26), the mechanisms controlling the differential usage of the splice sites remain unclear.

In the present work, performed on cells infected ex vivo with the closely related replication-competent Friend and Moloney MuLVs, we report for the first time the production of a large subgenomic transcript in a simple retrovirus. This novel RNA was generated from an alternative splice donor site, SD′, which is conserved among mammalian simple retroviruses, in combination with the *env* splice acceptor site. Mutations of SD′ in Friend and Moloney MuLVs affect the general splicing pattern of viral RNAs and reduce viral replication. Identification of this novel MuLV subgenomic RNA provides new insights into simple retrovirus functions.

MATERIALS AND METHODS

Mutagenesis and proviral constructs. The parental prototypic Friend MuLV strain 57 (16) and Moloney MuLV strain 8.2 (23) were used as permutated molecular clones with a single copy of the long terminal repeat (24). These clones provided the wild-type (wt) background sequences for the reconstitution of replication-competent Friend and Moloney mutants. Mutations were introduced by PCR with oligonucleotide-directed mutagenesis (11). The pMSD1/B plasmid carrying the entire Moloney MuLV sequence with the M1 mutation was previously described (1). The same strategy was used for construction of Friend F1, F2, and FDV mutants. All mutated fragments introduced in the wt parental MuLV were sequenced. Details of plasmid construction will be provided on request.

Cell culture, transfection, and infection. *Mus dunni* fibroblasts (Dunni cells) (12) were maintained in Dulbecco's modified Eagle's medium supplemented with glutamine (2 mM), penicillin, streptomycin, and 10% heat-inactivated fetal calf serum at 37°C. One microgram of wt or mutant DNA was transfected onto Dunni cells by the Lipofectamine method according to the instructions described by the manufacturer (Gibco BRL). Transfections were monitored by focal immunofluorescence assay (FIA) using anti-*env* monoclonal antibodies (25). Reverse transcriptase (RT) activity was measured by using a rapid assay as previously described (7). For preparation of mutant viral stocks, supernatants were collected from transfection experiments that led to confluently positive monolayers in less than 20 days, within the same time period as wt-transfected cells. Titration of viral stocks on Dunni cells was also performed by FIA. Average viral titers, expressed as infectious focus-forming units (FFU) per milliliter, were as follows: Friend, 10^5; F1, 6×10^2; F2, 7×10^3; FDV, 3×10^4; Moloney, 10^4; and M1, 2×10^3. To determine and compare precisely the levels of viral production by cells infected with wt or mutant viruses, a two-step method was used. First, Dunni cells were infected with serial dilutions of viral stocks in the presence of polybrene (8 μg/ml). After 2 or 3 days of infection, we determined by FIA the exact number of infected foci per dish, which varies linearly with the viral input in this assay (25). One tissue culture dish with approximately 600 to 800 FFU was selected. Supernatants corresponding to monolayers with the same number of foci were filtered through 0.45-μm-pore-size filters and used in a second round of infection on Dunni cells. Comparison of viral production was based on the number of FFU per milliliter determined in the second round of infection divided by the number of foci obtained in the first round of infection. In some experiments, RT activity assays were performed in parallel in order to quantify viral particle contents in supernatants produced by infected cells.

RNA analysis. Cells were infected with different wt and mutant viral strains and cultured in 10-cm-diameter plates for 4 days at 37°C. Viral RNA was isolated from viral particles essentially as described previously (14). Cells were washed twice with phosphate-buffered saline, and total RNA was extracted from cell pellets with TriReagent (Sigma) according to the manufacturer's instructions. The samples were treated with RNase-free DNase (RQ1; Promega) to remove DNA contamination. Cellular RNA concentrations were quantitated by measuring optical absorption at 260 nm.

For Northern blot analysis, 5 to 10 μg of cellular RNA were fractionated on denaturing formaldehyde agarose gels (14), blotted onto Hybond-N nylon, and UV cross-linked to the nylon. Viral transcripts were detected by hybridization with the *Xba*I-*Kpn*I MuLV fragment (nucleotides [nt] 5638 to 8327) radiolabeled by the random primer method (6) and radiography.

Semiquantitative RT-PCR was performed with the Expand reverse transcriptase and Expand long template PCR system (Boehringer Mannheim Biochemicals). Five micrograms of cellular RNA sample and sequential threefold dilutions were denatured in the presence of 220 ng of oligo$(dT)_{15}$ at 65°C for 10 min and chilled for 5 min at 4°C. RNA was reverse transcribed for 1 h at 42°C and shifted to 52°C for 30 min in a 20-μl reaction volume containing RT buffer, 10 mM deoxynucleoside triphosphate (dNTP) mix, 10 mM dithiothreitol DTT, 20 U of

* Corresponding author. Mailing address: Institut de Génétique Moléculaire de Montpellier II (IGMM), IFR 24, CNRS-UMR5535, Université Montpellier II, 1919, Rte. de Mende, F-34293 Montpellier Cedex 5, France. Phone: 33 (4) 67 61 36 40. Fax: 33 (4) 67 04 02 31. E-mail: mougel@igm.cnrs-mop.fr.

RNasin (Promega), and 50 U of Expand RT. The mixture was then inactivated at 95°C for 2 min and chilled at 4°C. One-fifth of each reaction mixture was used as the starting material for the different PCRs. Four combinations of oligonucleotide pairs, where "s" and "a" indicate the sense and antisense orientations, respectively, were used to detect specific MuLV transcripts. The positions of the transcriptional starts were as follows, with the sizes of the amplified products indicated in parentheses: s3350 and a3600 (250 bp) for full-length RNA detection, and s76 and a5620 (259 bp) for SD, s1450 and a5620 (276 bp) for SD′, and s6153 and a6418 (265 bp) for total MuLV RNAs. PCRs were carried out with 10 mM dNTP mix, PCR buffer, 1.5 U of Expand DNA polymerase mix, and 220 ng of each of the sense and antisense primers. Denaturation, annealing, and extension were performed at 94, 57, and 68°C, respectively. PCRs were performed on a RoboCycler Gradient 96 thermocycler (Stratagene) with 20 cycles for total, full-length, and *env* amplifications and 24 cycles for SD′ or SD″ amplifications. These cycles were preceded by a 5-min denaturation at 94°C and terminated by a 10-min extension at 68°C. Amplified products were electrophoresed on agarose gels, and bands were quantified by FluorImager (Molecular Dynamics). Experiments conducted in parallel with addition of a radiolabeled oligonucleotide were used to quantitate the amplified products by PhosphorImager (Molecular Dynamics), and there was a good correlation between the two methods.

Extensive amplifications (30 cycles) were also performed to obtain sufficient amounts of DNA for sequencing. Amplified DNA products was sequenced on an automatic sequencer (ABI PRISM 377; Perkin-Elmer) with the dye terminator cycle sequencing ready reaction kit (ABI PRISM) by following the recommendation of the manufacturer and using an oligonucleotide complementary to nt 5601 to 5620 of MuLV.

For RNase protection assays, 15 μg of total RNA were generally used. Riboprobe transcription was performed with linearized template plasmids according to standard procedures (3). The 274-nt Moloney riboprobe was generated from the SPMLV plasmid linearized with *Eco*RI and includes 5′ and 3′ non-MuLV vector sequences (3, 14). An SPFLV vector was derived after insertion of the Friend *Sac*I8273-*Bal*I213 homologous fragment in pGEM. The 274-nt Friend riboprobe was obtained after linearization of SPFLV with *Eco*RI. These probes should both yield a 214-nt genomic and a 205-nt spliced fragment after RNase digestion, as previously described (14). RNase protection products were quantitated by the PhosphorImager.

RESULTS

Identification of a novel MuLV RNA transcript. Total cellular RNA extracted from Dunni cells infected with Friend MuLV was examined by Northern blot hybridization using a probe complementary to the 3′ end of the Friend MuLV sequence. This yielded two expected major bands corresponding to the full-length genomic transcript (8.3 kb) and the single-spliced *env* RNA (3 kb) (Fig. 1). However, we noted an additional faint band, below the 28S RNA, corresponding to a potential 4- to 5-kb transcript. This faint band was more readily detected in the FDV mutant of Friend MuLV, which was obtained after introduction of two synonymous point mutations in the *gag* region (Fig. 2). Interestingly, the FDV mutations surround a potential 5′ splice site that is implicated in MuLV-driven rearrangements of the *c-myb* proto-oncogene (15, 21). In order to determine the precise nature of this new 4- to 5-kb RNA in replication-competent MuLV, extensive RT-PCR amplifications (30 cycles) were performed on two different strains of MuLV. We detected this novel RNA with both Friend and Moloney MuLV (Fig. 3). The sequence of the amplified fragment containing the splicing junction revealed the use of the alternative splice donor site mentioned above, designated here as SD′. SD′ is located in the 3′ third of the capsid-coding region in the *env* intron, at positions 1597 and 1596 of Friend and Moloney, respectively. The 3′ splice site used in concert with SD′ was located at position 5491 for Friend and 5490 for Moloney, corresponding to the canonical splice acceptor site (SA) that yields the single-spliced *env* RNA.

Effects of SD′ mutations on viral replication. To evaluate the influence of the SD′ sequence on the MuLV life cycle, we generated replication-competent MuLV mutants with distinct point mutations in this sequence. It is important to note that all the mutations maintained the wt Gag amino acid sequence. In the aforementioned FDV mutant, the two mutated nucleotides

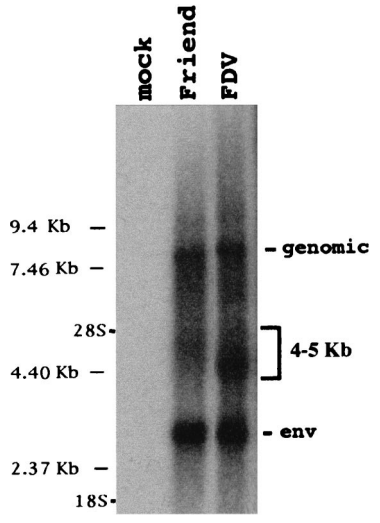

FIG. 1. Viral RNA species expressed in MuLV-infected cells. Cellular RNA from mock-infected cells or cells acutely infected with wt Friend MuLV or the FDV mutant (see Fig. 2) were analyzed by Northern blot hybridization with a radiolabeled probe complementary to the 3′ MuLV region (nt 5638 to 8327). This probe reveals the viral genomic RNA (8.3 kb), the single-spliced *env* RNA (3 kb), and a third RNA species (4 to 5 kb). Positions of RNA molecular size markers and 28S and 18S ribosomal RNAs are indicated.

also maintained the potential parental base-pairing of SD′ with the U1 snRNA consensus (Fig. 2). We generated two other Friend mutants, F1 and F2, and one Moloney mutant, M1, in which putative mismatches with U1 snRNA were introduced (Fig. 2). The Gag and Env precursor proteins and cleaved products were detected in all mutants, as assessed by immunoblotting (not shown). The infectivities of the mutant and wt strains were determined by monitoring cell surface envelope expression on newly infected cells by using the quantitative FIA (25) (Fig. 4), as well as by measuring the RT activity of the various supernatants (not shown). The former technique is a measure of protein production from the spliced *env* RNA while the latter reflects the production of RT by the unspliced *gag-pol* RNA. These two tests yielded similar results, indicating a significant reduction (ranging from 7- to 100-fold) in the infectivity observed with the different SD′ mutants (Fig. 4). The F1 and M1 mutants, which displayed the lowest potential base pairing with U1 snRNA, exhibited the lowest infectious ability. Interestingly, the replication capacity of the FDV mutant,

		No. of U1 mismatches
5′ SS consensus	C/A AG/GU G/A AGU	
	1581 1614	
Friend wt SD′	CUACAACACCCAACGAG/GUAGGAACCACCUAGUC	3
FDV	U----------/----------G	3
F1	----------/-AC-C----------	6
F2	----------/-C--A----------	5
	1580 1613	
Moloney wt SD′	UUACACCACCCAGGCAG/GUAGGAACCACCUAGUC	2
M1	----------/-AC-C----------	5
	204 212	
MuLV wt SD	GAG/GUAAGC	2

FIG. 2. Sequences of Friend and Moloney MuLV mutants in the SD′ region. Sequences of Friend (FDV, F1, and F2) and Moloney (M1) viruses containing changes in the SD′ region were aligned with the 5′ splice donor site (5′ SS) consensus sequence of U1 snRNA. The cleavage site is indicated by a slash mark. The nucleotide changes maintain the coding potential of the parental strains and are indicated for each mutant. For comparison, the sequence of the conserved canonical MuLV 5′ splice donor site (SD) is shown. The number of potential mismatches between each splice donor site and the U1 snRNA is on the right.

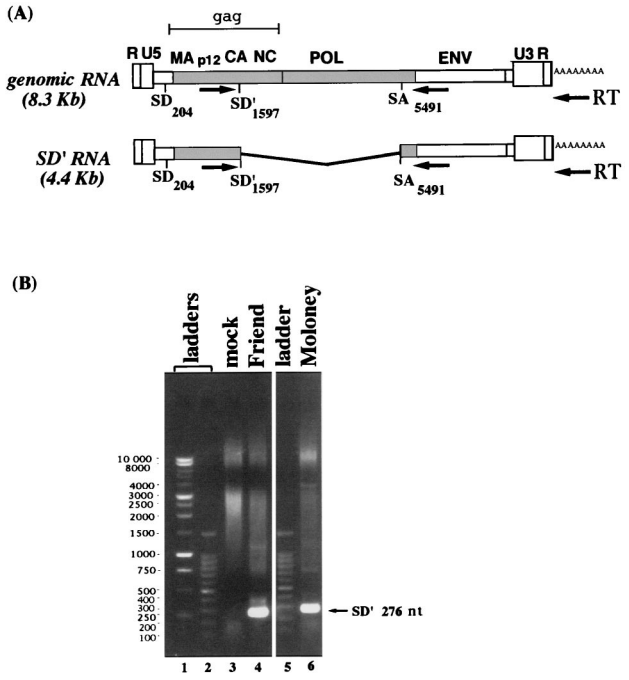

FIG. 3. Amplification of a new alternatively spliced MuLV transcript by RT-PCR. (A) Schematic structures of the unspliced genomic and alternatively spliced (SD′) RNA, including the canonical (SD), acceptor (SA), and alternative (SD′) splice sites. Nucleotides are numbered starting from the first nucleotide of R according to the Friend MuLV sequence. Also noted are the *gag* gene components, including the matrix (MA), capsid (CA), and nucleocapsid (NC). Arrows refer to the approximate positions of primers used for RT with the oligo(dT) primer and for PCR amplification. (B) RT-PCR was conducted on total RNA samples extracted from mock-infected cells (lane 3) or cells infected with either Friend (lane 4) or Moloney virus (lane 6). Reverse transcriptions were performed with oligo(dT), and PCRs were performed with oligonucleotides s1450 and a5620 as described in the Materials and Methods. The alternatively spliced SD′ RNA yielded an amplified product of 276 bp. After 30 cycles, amplified samples were loaded onto an agarose gel and stained with ethidium bromide. Lanes 1 and 2, 1-kb and 100-bp ladders, respectively.

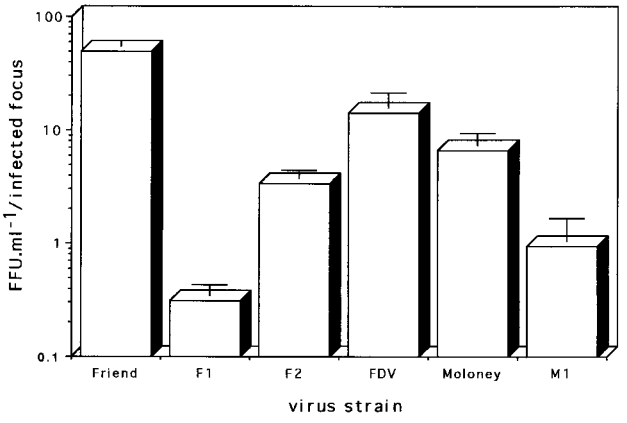

FIG. 4. Replication of wt and mutant viruses. FIA was used to quantitate infectious virions present in the supernatants harvested from cell cultures with the same number of wt or mutant MuLV-infected foci. Infectivities were performed at least three times for each virus in parallel and each test was performed in triplicate. Bars, the standard error of the mean of each series.

which maintained the parental U1 snRNA base pairing, was the least altered.

Effects of SD′ mutations on MuLV splicing. To evaluate whether the observed reduction in MuLV titers following mutation of the SD′ sequence was associated with an alteration in the alternative splicing efficiency, we next examined the splicing patterns of these mutants in infected cells. Semiquantitative RT-PCR was performed with total RNA extracted from de novo-infected Dunni cells. Full-length RNA, single-spliced *env* RNA, alternatively spliced RNA, and total MuLV transcripts were monitored with different combinations of oligonucleotide pairs (Fig. 5A). Although similar results were obtained when the initial RT reaction was performed with a specific MuLV or an oligo(dT) primer, we preferred the latter because it allowed amplification of the total cellular RNA independently of infection efficiency. The RT-PCR band obtained with the F1, F2, and M1 mutants migrated slightly slower than that detected with wt MuLV or FDV (Fig. 5A). Sequencing of the amplified product in F1, F2, and M1 revealed the recruitment of another cryptic donor site, AAG/GUAAA, designated here as SD″. It is present in both Friend and Moloney and is located 82 nt downstream of SD′. As for SD′, SD″ was used in conjunction with the SA canonical acceptor site. Therefore, impairment of SD′-U1 base pairing in these mutants resulted in the activation of a cryptic splice donor site (SD″).

For comparison purposes, the ratio of the amount of each transcript to the total level of MuLV RNA was determined and normalized to the ratio of the corresponding wt MuLV (Fig. 5B). Differences were evaluated by using the two-tailed Student *t* test and considered significant when probability values (*P*) were <0.05. Although semiquantitative RT-PCR does not allow the precise quantification of small differences in RNA expression, this method revealed dramatic differences in the relative amounts of alternatively spliced RNA species between mutant and wt MuLV. We observed a significant increase in the SD′ RNA level in cells infected with the FDV mutant ($P < 0.001$), in agreement with the initial observation made on Northern blots (Fig. 1). Also, the F1 and F2 Friend mutants harbored a much higher level of SD″ RNA than the equivalent M1 Moloney mutant (Fig. 5), indicating that elements, additional to a functional alternative SD′ site, influenced SD″ usage.

Since the F1 and F2 mutations appeared to decrease levels of the canonically spliced *env* RNA (Fig. 5B), a more direct quantification of *env* RNA levels was performed by using the RNase protection assay. Total cellular RNA was hybridized to a riboprobe that spans the MuLV canonical splice donor site (SD) at position 205 (Fig. 6A). RNase digestion yielded a 214-nt protected fragment derived from the unspliced RNA and the SD′ or SD″ alternatively spliced RNA species and a shorter 205-nt long fragment corresponding to the canonical SD-spliced *env* transcript (Fig. 6A). A reproducible decrease in *env* RNA levels was observed for all mutants, albeit to different extents, when compared to the respective wt strains ($P < 0.04$) (Fig. 6B and C).

Conservation of a potential alternative splice donor site in the capsid of mammalian simple retroviruses. *gag* sequences of replication-competent MuLV, feline, porcine, and simian C- and D-type retroviruses were aligned. This showed that a 5′ splice site consensus sequence, corresponding to a conserved putative SD′ site, is present approximately 100 nt upstream of the major homology region (MHR) (4) in the capsid-coding gene (Fig. 7). Interestingly, the GU dinucleotide immediately adjacent to the cleavage site, which is present in almost all mammalian pre-mRNA introns (10), was strictly conserved among these viral sequences.

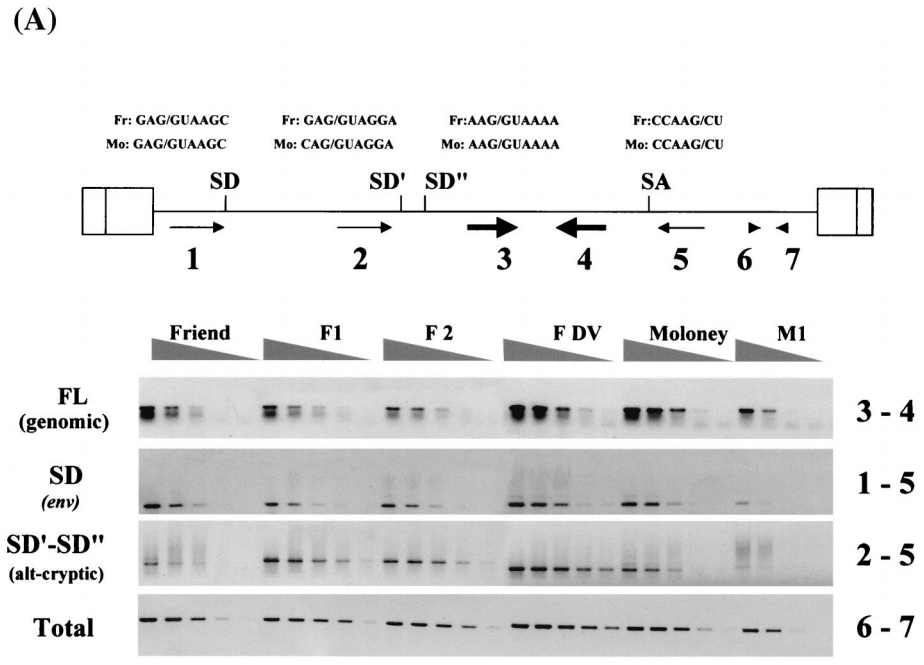

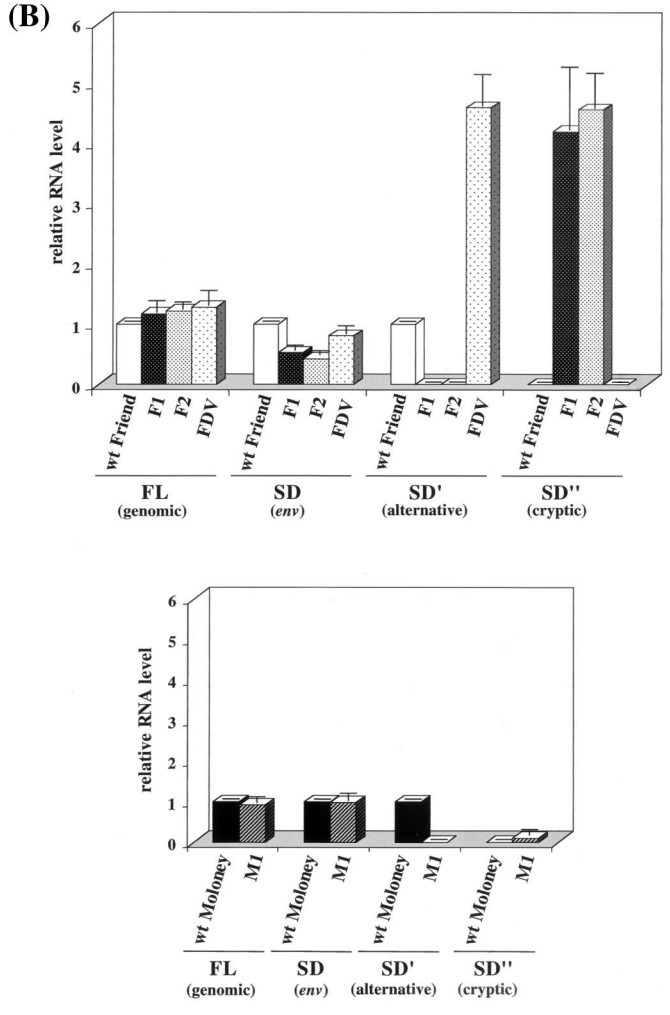

FIG. 5. Effect of SD′ mutations on MuLV splicing. The different RNA species were detected by semiquantitative PCRs (20 to 24 cycles) performed on threefold dilutions of each sample. The amplified products were run onto agarose gels containing ethidium bromide. (A) Schematic MuLV genome map indicating the splice donor (SD, SD′, and SD″) and acceptor (SA) sites. The corresponding sequences in Friend (Fr) and Moloney (Mo) are shown in the upper panel. Approximate positions of the primers used to amplify the different RNA species are identified by the numbered arrows. Each viral RNA species detected is indicated on the left side of the gel, with the corresponding oligonucleotide pairs identified by numbers on the right. Note that the main products amplified from the F1, F2, and M1 mutants correspond to usage of the cryptic SD″ and exhibit slower migration relative to products arising from usage of the alternative SD′ in the wt and FDV. (B) Quantification of the different RNA species was determined by a FluorImager. For each virus, at least two RNA preparations were isolated and subjected to three to six semiquantitative RT-PCR analyses. For each RNA species, the RNA levels are expressed as the ratio of the value obtained after amplification with the specific oligonucleotide pair divided by the total RNA value obtained by amplification with primers 6 and 7. Final RNA levels are represented after normalization to levels of the corresponding wt strain (± standard error of the mean). Note that both wt Friend and Moloney, as well as the FDV mutant, produced alternatively SD′ spliced RNA, while F1, F2, and M1 mutants displayed a spliced RNA resulting from the activation of the SD″ cryptic splice site.

DISCUSSION

We have identified a new 4.4-kb RNA transcript produced by two prototypic strains of MuLV. This novel RNA results from splicing between an alternative splice donor site, SD′, located in the capsid-coding region, and the canonical *env* splice acceptor site. Although in vivo studies of Moloney MuLV-induced promonocytic leukemia have shown that the recruitment of an SD′ sequence produces a rearranged truncated *c-myb* gene upon insertional mutagenesis (8, 21), this is the first report demonstrating that a second spliced RNA is produced during the life cycle of a replication-competent simple retrovirus. Moreover, we found that an SD′ sequence is present at a similar position in the capsid-coding gene of all the replication-competent MuLV, feline, porcine, and simian C-type retroviruses we examined. This conserved feature also extended to the more distantly related simian D-type oncoviruses. It will be interesting to determine whether an additional homologous subgenomic transcript is also present in these

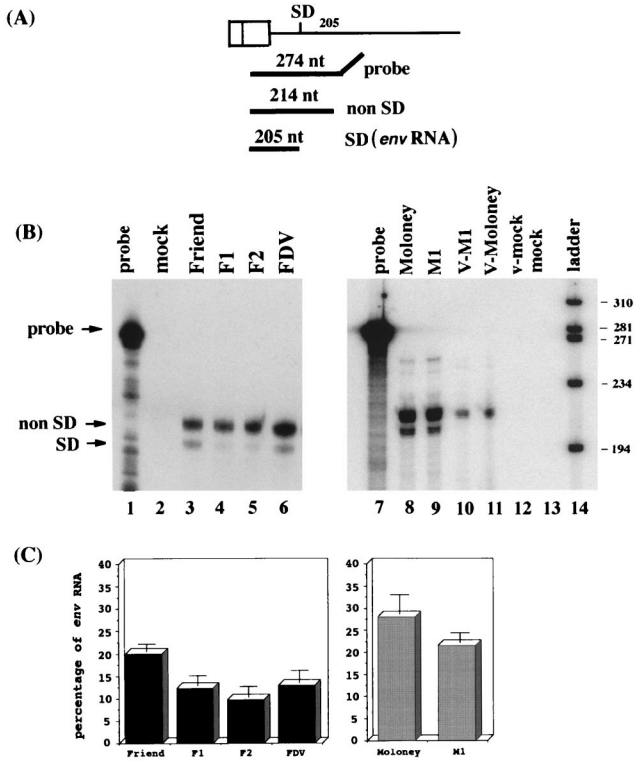

FIG. 6. Quantification by RNase protection of the canonical *env* transcript level in MuLV-infected cells. (A) Friend and Moloney transcripts were detected by RNase protection with the uniformly labeled antisense SPFLV or SPMLV probes, respectively (see Materials and Methods), which overlap the canonical SD site. Hybridization of the 274-nt probe to viral RNA species that are not spliced at the canonical SD site (full length, SD′, and SD″ RNA) yields a protected 214-nt fragment, while canonically spliced *env* RNA yields a protected 205-nt fragment. (B) RNase protection assays were carried out with 15 μg of total cellular RNA (lanes 2 to 6, 8, 9, and 13) and RNA extracted from 10% total virus pelleted medium from infected or mock-infected cell monolayers (lanes 10 to 12). The positions of the probe and the protected fragments corresponding to canonically spliced *env* RNA (SD) as well as the noncanonically spliced RNAs (non SD) are indicated by arrows. The size markers (lane 14) consist of end-labeled ϕX174 *Hae*III DNA fragments. (C) Quantification of RNase protection assays. For each series, the percentage of *env*-protected fragments versus the total of protected signals is represented (± standard of the mean). Each value corresponds to the average of at least three measurements performed on different RNA preparations.

		1595	1602
	5′ SS consensus	C/A AG	GU G/A AGU
Murine			
	Friend-MuLV	g--	--Ag-a
	Moloney-MuLV	C--	--Ag-a
	RadLV	A--	--Ag-a
	Cas-Br-E	g--	--Ag-a
	N-tropic WNB5	g--	--Ag-a
	B-tropic WNB5	A--	--Ag-a
	AKV	g--	--Ag-a
	polytropic MCF	A--	--Ag-a
Feline			
	FeLV-A	C--	--Ag-g
	FeLV-B	C--	--Ag-g
primate	Type C		
	BaEV	A--	--AA-g
	GaLV	C--	--Ag-g
	Type D		
	MPMV	C--	--uc-g
	SRV-Pc	C--	--A-u-
porcine	endogenous porcine	A--	--Ag-a

FIG. 7. Conservation of the SD′ site. Sequence alignment of a putative SD′ site in the capsid-coding region of a series of replication-competent mammalian types C and D retroviruses. The 5′ splice donor site consensus sequence (5′ SS) is shown on top, with the potential splicing cleavage site indicated by a vertical line. All sequences were located approximately 100 nt upstream of the capsid major homology region. Numbering is according to the Friend-MuLV 57 sequence. Lower-case letters indicate mismatches between the 5′SS consensus and the viral sequence. Abbreviations and strains correspond to the following retroviruses. (i) MuLVs: Friend-MuLV, strain 57; Moloney-MuLV, strain 8.2; RadLV, radiation leukemia virus; Cas-Br-E, Lake Casitas brain E neurotropic virus; WNB5, the N- and B-tropic clones of the WN1802 isolate; and AKV, from clone AKR 623 of endogenous virus from the AKR mouse strain. All of the above are ecotropic MuLVs. MCF, clone MCF1233 of the polytropic mink cell focus-inducing viruses. (ii) Feline leukemia viruses: FeLVA and FeLVB, strains A and B. (iii) Primate simple retroviruses: simian type C retroviruses include BaEV, baboon endogenous virus, and GaLV, gibbon ape leukemia virus. Simian type D retroviruses include MPMV, Mason-Pfizer monkey virus, and SRV-Pc, a baboon simian retrovirus-like isolate. (iv) Porcine endogenous virus: a human-tropic C-type porcine endogenous retrovirus.

retroviruses, as already suggested in a previous report with the gibbon ape leukemia virus (5).

This new 4.4-kb RNA was weakly detectable by Northern blot analysis of RNA from cells infected with the wt Friend strain, suggesting a low level of production and/or a potential instability of the mature SD′ transcript. Since the synonymous mutations introduced in the FDV mutant flanked the SD′ site and increased the SD′ RNA level, it is likely that potential local RNA structures also modulate splicing at this site.

Production of two spliced RNAs from a single precursor and maintenance of the full-length RNA pool require incomplete splicing. According to our results, production of the alternatively spliced SD′ RNA might play an important role in splicing regulation in MuLV simple retroviruses. Thus, when SD′ splicing was maintained (wt and FDV), cryptic splicing at SD″ was not detected and mutations in Friend-MuLV that activated the alternative SD′ or cryptic SD″ were accompanied by a decreased production of the canonical *env* spliced RNA (FDV, F1, and F2). However, a strict competition model between these sites cannot account for the splicing pattern observed in the Moloney MuLV strains, since a significant impairment of alternative splicing in the M1 mutant did not lead to increased levels of the *env* RNA. Furthermore, usage of these potentially competing sites did not strictly correlate to U1 base pairing. For instance, although both SD″ and the canonical SD site harbored two potential mispairings with U1, an SD″ RNA remained undetectable in the wt viral strains. Therefore, other parameters, such as neighboring (14) or distant RNA structures (13), likely influence the splicing balance. This underlines the usefulness of full-length viruses in unraveling regulatory elements involved in the modulation of RNA expression.

Since decreased levels of infection observed with the mutants resulted from synonymous mutations in the SD′ region, this was the first demonstration of a *cis*-acting effect of the capsid region in the context of a replication-competent retrovirus. The severe drop observed in replication abilities of the F1, F2, and M1 mutants could result from a negative effect of the newly produced SD″ RNA, loss of the SD′ RNA, or alteration of the splicing balance. Nevertheless, results obtained with the FDV mutant, which harbors a high level of SD′ RNA and a slightly altered viral titer, suggest that SD′ usage is required for a balanced splicing profile and optimal replication.

In addition, the coding capability of the SD′ RNA might be directly involved in the increased level of infectious retroviral

particles. The alternatively spliced SD′ RNA was polyadenylated, as shown by its presence in the poly(A)$^+$ RNA fraction (not shown), and could be reverse transcribed with an oligo(dT) primer. Also, the SD′ RNA presents a large coding potential, with multiple translation initiation codons; these include initiation codons used in the *glycogag*, *gag*, and *env* open reading frames, which are active in the full-length or canonically spliced mRNA, as well as the initiation codon in the capsid that is used in the chimerical *gag-myb* transcripts (19, 26). These many putative initiation codons, placed in the context of new *gag* and *env* open reading frames, provide the potential for new MuLV translational products. Identification of this novel alternatively spliced MuLV RNA at a site that is highly conserved among types C and D mammalian oncoviruses provides new avenues of investigation on the influence of new RNA species in replication of simple retroviruses.

ACKNOWLEDGMENTS

We thank laboratory members past and present, including F. Kim, K. Beemon, J. Richardson, S. Orsoni, B. Hohl, and L. Drumright for help and advice during the course of this work and N. Taylor, R. Hipskind, and J. M. Blanchard for critical reading of the manuscript.

This work was supported by grants no. 9521 and 4066 from the Association pour la Recherche sur le Cancer (to M.M. and M.S.) and by successive grants from CNRS (ATIPE virology program) and the Fondation pour la Recherche Médicale and a Philippe Foundation award (to M.S.). M.M. and M.S. are supported by the Centre National de la Recherche Scientifique (CNRS) and the Institut National de la Santé et de la Recherche Médicale (INSERM), respectively. J.D. was supported by a fellowship from the French government (MENRT).

REFERENCES

1. **Audit, M., J. Dejardin, B. Hohl, C. Sidobre, T. J. Hope, M. Mougel, and M. Sitbon.** 1999. Introduction of a *cis*-acting mutation in the capsid-coding gene of Moloney murine leukemia virus extends its leukemogenic properties. J. Virol. **73:**10472–10479.
2. **Barker, C. S., S. E. Bear, T. Keler, N. G. Copeland, D. J. Gilbert, N. A. Jenkins, R. S. Yeung, and P. N. Tsichlis.** 1992. Activation of the prolactin receptor gene by promoter insertion in a Moloney murine leukemia virus-induced rat thymoma. J. Virol. **66:**6763–6768.
3. **Barklis, E., R. C. Mulligan, and R. Jaenisch.** 1986. Chromosomal position or virus mutation permits retrovirus expression in embryonal carcinoma cells. Cell **47:**391–399.
4. **Craven, R. C., A. E. Leure-duPree, R. J. Weldon, Jr., and J. W. Wills.** 1995. Genetic analysis of the major homology region of the Rous sarcoma virus Gag protein. J. Virol. **69:**4213–4227.
5. **Eiden, M., C. D. Trainor, and M. S. Reitz.** 1986. Gibbon ape leukaemia virus RNA in leukaemic T-lymphoid cell lines: expression of a novel RNA transcript. J. Gen. Virol. **67:**1455–1460.
6. **Feinberg, A. P., and B. Vogelstein.** 1983. A technique for radiolabeling DNA restriction endonuclease fragments to high specific activity. Anal. Biochem. **132:**6–13.
7. **Goff, S., P. Traktman, and D. Baltimore.** 1981. Isolation and properties of Moloney murine leukemia virus mutants: use of a rapid assay for release of virion reverse transcriptase. J. Virol. **38:**239–248.
8. **Gonda, T. J., S. Cory, P. Sobieszczuk, D. Holtzman, and J. M. Adams.** 1987. Generation of altered transcripts by retroviral insertion within the c-myb gene in two murine monocytic leukemias. J. Virol. **61:**2754–2763.
9. **Hwang, L. S., J. Park, and E. Gilboa.** 1984. Role of intron-contained sequences in formation of moloney murine leukemia virus env mRNA. Mol. Cell. Biol. **4:**2289–2297.
10. **Jackson, I. J.** 1991. A reappraisal of non-consensus mRNA splice sites. Nucleic Acids Res. **19:**3795–3798.
11. **Kunkel, T. A.** 1985. Rapid and efficient site specific mutagenesis without phenotypic selection. Proc. Natl. Acad. Sci. USA **82:**488–492.
12. **Lander, M. R., and S. K. Chattopadhyay.** 1984. A *Mus dunni* cell line that lacks sequences closely related to endogenous murine leukemia viruses and can be infected by ecotropic, amphotropic, xenotropic, and mink cell focus-forming viruses. J. Virol. **52:**695–698.
13. **Lewis, J. D., S. I. Gunderson, and I. W. Mattaj.** 1995. The influence of 5′ and 3′ end structures on pre-mRNA metabolism. J. Cell. Sci. Suppl. **19:**13–19.
14. **Mougel, M., Y. Zhang, and E. Barklis.** 1996. *Cis*-active structural motifs involved in specific encapsidation of Moloney murine leukemia virus RNA. J. Virol. **70:**5043–5050.
15. **Nason-Burchenal, K., and L. Wolff.** 1993. Activation of c-*myb* is an early bone marrow event in murine model for acute promonocytic leukemia. Proc. Natl. Acad. Sci. USA **90:**1619–1623.
16. **Oliff, A. I., G. L. Hager, E. H. Chang, E. M. Scolnick, H. W. Chan, and D. R. Lowy.** 1980. Transfection of molecularly cloned Friend murine leukemia virus DNA yields a highly leukemogenic helper-independent type C virus. J. Virol. **33:**475–486.
17. **Oshima, M., T. Odawara, T. Matano, H. Sakahira, Y. Kuchino, A. Iwamoto, and H. Yoshikura.** 1996. Possible role of splice acceptor site in expression of unspliced gag-containing message of Moloney murine leukemia virus. J. Virol. **70:**2286–2295.
18. **Rabson, A. B., and B. J. Graves.** 1997. Synthesis and processing of viral RNA, p. 205–262. *In* J. M. Coffin, S. H. Hughes, and H. E. Varmus (ed.), Retroviruses. CSH Laboratory Press, New York, N.Y.
19. **Shen-Ong, G. L. C., H. C. Morse III, M. Potter, and J. F. Mushinski.** 1986. Two modes of c-*myb* activation in virus-induced mouse myeloid tumors. Mol. Cell. Biol. **6:**380–392.
20. **Shen-Ong, G. L., M. Potter, J. F. Mushinski, S. Lavu, and E. P. Reddy.** 1984. Activation of the c-myb locus by viral insertional mutagenesis in plasmacytoid lymphosarcomas. Science **226:**1077–1080.
21. **Shen-Ong, G. L. C., and L. Wolff.** 1987. Moloney murine leukemia virus-induced myeloid tumors in adult BALB/c mice: requirement of c-*myb* activation but lack of v-*abl* involvement. J. Virol. **61:**3721–3725.
22. **Shin, S., and D. L. Steffen.** 1993. Frequent activation of the lck gene by promoter insertion and aberrant splicing in murine leukemia virus-induced rat lymphomas. Oncogene **8:**141–149.
23. **Shoemaker, C., S. Goff, E. Gilboa, M. Paskind, S. W. Mitra, and D. Baltimore.** 1980. Structure of a cloned circular Moloney murine leukemia virus DNA molecule containing an inverted segment: implications for retrovirus integration. Proc. Natl. Acad. Sci. USA **77:**3932–3936.
24. **Sitbon, M., H. Ellerbrok, F. Pozo, J. Nishio, S. F. Hayes, L. Evans, and B. Chesebro.** 1990. Sequences in the U5-gag-pol region influence early and late pathogenic effects of Friend and Moloney murine leukemia viruses. J. Virol. **64:**2135–2140.
25. **Sitbon, M., J. Nishio, K. Wehrly, D. Lodmell, and B. Chesebro.** 1985. Use of a focal immunofluorescence assay on live cells for quantitation of retroviruses: distinction of host range classes in virus mixtures and biological cloning of dual-tropic murine leukemia viruses. Virology **141:**110–118.
26. **Tantravahi, R., H. Dudek, G. Patel, and E. P. Reddy.** 1996. Murine myeloid leukemic cells with disrupted myb loci show splicing anomalies that account for heterogeneous sizes in myb proteins. Oncogene **13:**1187–1196.